Applied Chemical Engineering (2026) Volume 9 Issue 4 ISSN: 2578-2010 (O)
doi: 10.59429/ace.v9i4.5962

RESEARCH ARTICLE

Electron Scattering Form Factors using the Bohr–Mottelson Collective Model for 17O, 19O, and 25Al Nuclei

Zahraa Hussein, Khalid S. Jassim*, Farah J. Hamood

Department of Physics, College of Education for Pure Science, University of Babylon,, Iraq

***Corresponding author:** Khalid S. Jassim, Zahraahhuuss20@gmail.com

ABSTRACT

The magnetic electron scattering form factors of the 17O, 19O, and 25Al nuclei were investigated using the Bohr–Mottelson collective model within the framework of the nuclear shell model. Calculations were performed in the SDPF model space using the NuShellX@MSU code, while harmonic oscillator wave functions were employed to describe the single-particle states. The one-body density matrix elements (OBDMs) were obtained from the shell-model eigenvectors and used in the calculation of elastic and inelastic magnetic form factors. The contributions of the M1, M3, and M5 multiple components were analyzed for the selected transitions. The calculated form factors were compared with the available experimental data. Good agreement was obtained for the 17O nucleus over most of the momentum-transfer region, demonstrating the capability of the Bohr–Mottelson model to describe magnetic electron scattering observables in light nuclei. The results provide additional insight into the nuclear structure and electromagnetic transition properties of Sd-shell nuclei.

Keywords: Single particle density, Forma factors, electron scattering, Transverse magnetic form factors

ARTICLE INFO

Received: 25 March 2026
Accepted: 25 June 2026
Available online: 05 November 2026

COPYRIGHT

Copyright © 2026 by author(s).
Applied Chemical Engineering is published by Arts and Science Press Pte. Ltd. This work is licensed under the Creative Commons Attribution-NonCommercial 4.0 International License (CC BY 4.0).
https://creativecommons.org/licenses/by/4.0/

1. Introduction

Several microscopic theories have been used to explore the mechanism of nuclear excitation. To understand the possibilities of interaction between some nuclei, it is necessary to analyze and interpret nuclear reactions [1]. Given that the electron can be easily accelerated, this method is considered the best way to express the charge distribution in the nucleus through electron scattering. To clearly and accurately explain a larger group of phenomena, the appropriate residual interaction is chosen [2]. It is known that there are two types of scattering: the first type is called elastic electron scattering, where this type studies the properties of the ground state, for example, static charge and magnetic distribution. The electron scattering refers to the process in which an electron in a beam interacts with an atom in a sample, resulting in a change in direction and minimal loss of energy. This interaction is primarily due to Coulomb attraction between the approaching electron and the nucleus of the. In the process of electron transfer, a small part of its energy will be equivalent to the energy transferred to the nucleus, putting it in an excited state with a final energy lower than its initial energy. The second type of scattering is known as inelastic electron scattering It is a type of scattering between two particles (such as electrons, neutrons, or photons) in which an exchange of energy occurs between the scattering particle and the target body. [3]. It is well known that

nuclear models are a powerful and important tool for studying the internal structure of nuclei. This model has greatly helped us understand the internal structure of the nucleus. Despite its simplicity, it was effective in explaining a wide range of nuclear phenomena, notably spin, magnetized moments, and atomic spectra [4]. The shape factor, which reflects the core charge distribution, is used in conjunction with the cross-sectional area to calculate the core size [5]. Another factor is added to the cross-sectional area F(q), and based on the same distributions, its actual size can be found [6]. In this work, we use distorted nuclei and follow the electron scattering formula in their study. This graphic depicts the scattering caused by the nuclear charge density through the shape of the scattering of the operating electron. The dispersion derived from the nuclear current density. is described by the transverse form factor F(q), which includes all nuclear descendants. [7] Khalid et al. have done many studies and calculations based on the nuclear shell model and everything related to the nuclear structure of different nuclei in the p, sd, fp model spaces through the nuclear shell structure model and electron scattering calculations - in the sdpf space, the longitudinal form factor was investigated [8]. In this study, the electron scatter form factors, as well as the sdpf space, have been determined using the Bohr-Mottelson (BM) model of some light nuclei: ^{17}O, ^{19}O, ^{25}Al nuclei. The potential used in this work is (HO) in which it was used to calculate the matrix waveform for the single particle of ^{25}Al, ^{19}O nuclei without experimental results. In the case of the oxygen nuclear isotope ^{17}O, its scattering electron coefficients were calculated and compared to data from experiments, and the experimental and theoretical results for pairing agreed. Despite the extensive investigations of electron scattering form factors in sd-shell nuclei, detailed studies of the magnetic form-factor contributions in ^{17}O, ^{19}O, and ^{25}Al within the Bohr–Mottelson collective framework remain limited.[9] These nuclei are of particular interest because they provide valuable information about the interplay between single-particle and collective nuclear degrees of freedom.[10] Therefore, the present work aims to calculate and analyze the magnetic form factors of these nuclei using the Bohr–Mottelson model and shell-model calculations in the SDPF space and to compare the theoretical predictions with the available experimental data.[11]

2. Theoretical Part

Nuclear shell structure model provided the first fundamental mechanical image of the nucleus. The shell model is used as an approximation for the electrical structure of an atom. It is sensitive to the nucleons' angular momentum [12]. The name refers to the experimental relevance of some nuclear data outputs. The shell model describes the system as a collection of discrete particles that move in finite orbits in reaction to the rest of the system. Each orbital has distinct energy, angular momentum, and parity [13]. Since Mayer and Jensen introduced it the nuclear shell theory has proven to be an effective tool for comprehending underlying nuclear structure. The nuclear shell model's basic and important properties include the independence of the model assumption, the utilization of genuine nucleon-nucleon interactions, and the same Hamiltonian for many types of eigenstates and nuclei [14]. Digitization of the Hamiltonian matrix allows these complex applications to be accurately considered for digital matrix configurations. Considering these complex configurations for various applications, the microscopic derivative of the five-dimensional collective quadrupole Hamiltonian is as follows:

$$\hat{H}_{coll} = \hat{T}_{vib} + \hat{T}_{rot} + V(\beta, \gamma) \quad (1)$$

Here, the term is vibrational kinetic energy $\hat{T}_{vib}$. is defined as. [15,16]

$$\hat{T}_{vib} = -\frac{1}{2D}\left(\frac{1}{\beta^4}\frac{\partial}{\partial\beta}\beta^4\frac{\partial}{\partial\beta} + \frac{1}{\beta^2\ sin(3\gamma)\,\partial_\gamma}\frac{\partial}{\partial\gamma}sin(3\gamma)\frac{\partial}{\partial\gamma}\right)$$

In addition, the concept of rotational energy is defined as.[13],

$$\hat{T}_{rot} = \sum_{k=1}^{3} \frac{\hat{I}_k^2}{2J_k(\beta,\gamma)} \quad (2)$$

Five curved coordinates are used to express the classical Hamiltonian equation (1). (β, γ) linear transformation relates the three Euler angles. with φk as well as their time derivatives. We can use the Pauli version. For quantization using bent dimensions The Schrödinger equation is for the set [15,16].

$$\hat{T}_{vib} + \hat{T}_{rot} + V(\beta,\gamma)\Psi_{\alpha IM}(\beta,\gamma,\Omega) \quad (3)$$

The combined wave function in a lab frame, Ψ_αIM (β, γ,Ω), is a function of β, γ and α of the set Among the three Euler angles Ω. Eigen modes with identical numbers for I and M are distinguished by They are projected onto the z-axis in the testing frame. M and α, defined by the total angular momentum I. With the rotating wave function $\mathcal{D}^I_{MK}$, they are written as [15,16],

$$\Psi_{\alpha IM}(\beta,\gamma,\Omega) = \sum_{K=even} \Phi_{\alpha IM}(\beta,\gamma)\langle\Omega|IMK\rangle \quad (4)$$

$$\langle\Omega|IMK\rangle = \sqrt{\frac{2I+1}{161\pi^2(1+\delta_{k0})}}\left[D^I_{MK}(\Omega) + (-1)^i D^I_{M-k}(\Omega)\right] \quad (5)$$

A vibrating The wave acts in a fixed bodily frame.$\Phi_{\alpha IK}(\beta,\gamma)$, are normalized as [20]:

$$\int d\beta d\gamma \sqrt{G(\beta,\gamma)}|\Phi_{\alpha I}(\beta,\gamma)|^2 = 1 \quad (6)$$

Where

$$|\Phi_{\alpha I}(\beta,\gamma)|^2 = \sum_{k=even}|\Phi_{\alpha I}(\beta,\gamma)|^2 \quad (7)$$

The size of the A component was provided b$\sqrt{G(\beta,\gamma))}$ dγdβ with

$$G(\beta,\gamma) = 4\beta^8 W(\beta,\gamma)R(\beta,\gamma)sin^2(3\gamma) \quad (8)$$

The conditions needed to solve the group Schrödinger equation and The symmetries of the group wave functions are examined in detail in the references [17,18].

The eigenvalue equation for vibrational wave functions can be obtained by inserting (2.34) into the collective Schrödinger equation (3) [14].

$$\left[\widehat{T_{vib}} + V(\beta,\gamma)\right]\Phi_{\alpha IK}(\beta,\gamma) + \sum_{k=even}\left\langle IMK\middle|\widehat{T_{rot}}\middle|IMK\right\rangle \Phi_{\alpha Ik}(\beta,\gamma) = E_{\alpha I}\Phi_{\alpha Ik}(\beta,\gamma) \quad (9)$$

The quantum spectrum and collective wave functions are obtained by solving this equation. The electromagnetic transition probabilities among the collective excited states are then easily calculated. The well-known multiple decomposition provides the shape factors of the electron scattering [19].

$$F_l^2(q) = \frac{4\pi}{z^2}\frac{1}{2J_i}\sum_{J\geq 0}\left|\left\langle J_f\middle\|\hat{T}_J^{col}\middle\|J_i\right\rangle\right|^2 \quad (10)$$

where $T_J^{col.}(q)$ The states are the Coulomb multiple operators. J_I and J_f are, respectively, the nucleus's initial and ultimate states, and (J) is the multipolarity. The double bar ⟨‖ ⟩This indicates that the matrix spice decreases in rotation space . The minimum matrix component of the necessary operator T_Λ^η Each of the density matrix's components are combined to form a body.

$$\langle J_f \| \hat{T}^{\eta}_{J,t_z} \| J_i \rangle = \sum_{a,b} OBDM^{J,t_z}(J_i,J_f,a,b) \langle a \| \hat{T}^{col}_{J,tz} \| b \rangle, \tag{11}$$

where t_z=1/2 in the case of proton and -1/2 with neutron communities. J_I and J_f The initial and final states of the nucleus are multipolar. The Twin Bar ⟨‖ ⟩. This means that, the matrix that is a component within spin area is reduced. The final and starting states determine and affect the one-particle states. respectively [20].

$$|a\rangle = |n_a l_a\rangle |j_a m_a\rangle \tag{12}$$

$$|b\rangle = |n_b l_b\rangle |j_b m_b\rangle \tag{13}$$

In which $n_a(n_b)$The primary quantum value is , $l_a(l_b)$The orbital angular momentum quantum number is, j_a (j_b) The total of the angular component numbers of a single particle is m_a (m_b), respectively. The estimate of j_a (j_b) respectively. Reduction of the one-particle matrix element of its initial inter-element longitudinal operator (n_b, l_b, jb) and last (n_a, la, ja) states the nucleus are:

$$\langle n_a l_a j_a \| T_{J,t_z}(q) \| n_b l_b j_b \rangle\rangle = e(t_z) \langle n_a l_a | j_J(qr) | n_b l_b \rangle \left\langle l_a \frac{1}{2} j_a \| Y_J(\Omega_r) \| l_b \frac{1}{2} j_b \right\rangle \tag{14}$$

$$\langle l_a \frac{1}{2} j_a \| Y_J(\Omega_r) \| l_b \frac{1}{2} j_b \rangle \tag{15}$$

$$= \frac{1}{2}(-1)^{l_a+\frac{1}{2}} [1 + (-1)^{l_a+J+l_b}] \sqrt{\frac{(2j_a+1)\,(2j_b+1)(2J+1)}{4\pi}} \begin{pmatrix} j_a & J & j_b \\ 1/2 & 0 & -1/2 \end{pmatrix}$$

The transition amplitude of is the spherical Bessel functions [21]:

$$\langle n_a l_a | j_J(qr) | n_b l_b \rangle = \int_0^\infty dr\, r^2 R_{n_a l_a}(r)\, R_{n_b l_b}(r)\,, \tag{16}$$

where the radially component of the single-particle wave function $R_{nl}(r)$. Using the (HO) potential of the harmonic oscillator, this is characterized by the size parameter

TABLE OF SYMBOLS USED IN THE EQUATIONS

Symbol	Meaning (English)	Description
$\|a\rangle$, $\|b\rangle$	Basis states	Two basis states of the nuclear system.
$\|n_a l_a\rangle$, $\|n_b l_b\rangle$	Initial states	Initial inter-element longitudinal states.
$\|n_a l_a, j_a m_a\rangle$	Initial total state (a)	State with quantum numbers n_a, l_a, j_a, m_a.
$\|n_b l_b, j_b m_b\rangle$	Initial total state (b)	State with quantum numbers n_b, l_b, j_b, m_b.
n_a , n_b	Principal quantum numbers	Radial (principal) quantum numbers.
l_a , l_b	Orbital angular momentum quantum numbers	Orbital angular momentum quantum numbers.
j_a , j_b	Total angular momentum quantum numbers	Total angular momentum quantum numbers.
m_a , m_b	Magnetic quantum numbers	The total projection quantum numbers.
$\langle n_a l_a j_a m_a \|\hat{T}_J\| n_b l_b j_b m_b\rangle$	Matrix element	One-particle matrix element of the operator $\hat{T}_J$ between the two states.
e	Electron charge	Charge of the electron.
$e(\tau_z)$	Isospin factor	Depends on the third component of isospin τ_z.
q	Momentum transfer	Magnitude of the momentum transfer.
r	Radial coordinate	Distance (radial coordinate).
Ω_r	Solid angle	Solid angle in spherical coordinates.
$Y_J^M(\Omega_r)$	Spherical harmonic	Spherical harmonic function.
j_a , j_b	Angular momenta	Total angular momenta in the bra and ket.
$\begin{pmatrix} j_a & J & j_b \\ 1/2 & 0 & -1/2 \end{pmatrix}$	Wigner 3-j symbol	Wigner 3-j symbol (angular momentum coupling coefficient).
$(2j_a+1)(2j_b+1)(2J+1)$	Degeneracy factor	Product of the dimensions $(2j+1)$ factors.
4π	Solid angle normalization	Normalization factor from angular integration.
$(-1)^{l_a+\frac{1}{2}}$	Phase factor	Phase depending on l_a.
$(-1)^{j_b+\frac{1}{2}}$	Phase factor	Phase depending on j_b.
$\langle l_a \frac{1}{2} j_a \\|Y_J(\Omega_r)\\| l_b \frac{1}{2} j_b\rangle$	Reduced matrix element	Reduced matrix element of the spherical harmonic.
$\langle qr\rangle$	Radial integral variable	Radial coordinate in the integral.
$R_{n_a l_a}(r)$	Radial wave function	Radial wave function of the initial state a.
$R_{n_b l_b}(r)$	Radial wave function	Radial wave function of the initial state b.
$\hat{T}_J(qr)$	Transition operator	Transition operator of multipolarity J.
$j_l(x)$	Spherical Bessel function	Spherical Bessel function of order l.

Symbol	Meaning (English)	Description
$\int d\beta d\gamma \sqrt{G(\beta,\gamma)} \\|\Phi_{\alpha I}(\beta,\gamma)\\|^2 = 1$	Normalization condition	Normalization condition of the collective wave function.
$\Phi_{\alpha I}(\beta,\gamma)$	Collective wave function	Collective wave function depending on β, γ.
α	Band index	Label for different collective bands.
I	Total angular momentum	Total angular momentum quantum number.
$G(\beta,\gamma)$	Metric (mass) function	Function appearing in the collective Hamiltonian measure.
$B^M(\beta,\gamma)$	Mass parameter	Mass parameter for β vibrations.
$B(\beta,\gamma)$	Mass parameter	Mass parameter for γ vibrations.
$\sin^2(3\gamma)$	Geometrical factor	Geometrical factor from the kinetic energy operator.
$\hat{H}_{\text{vib}}$	Vibrational Hamiltonian	Vibrational kinetic energy operator.
$\hat{H}_{\text{rot}}$	Rotational Hamiltonian	Rotational kinetic energy operator.
$V(\beta,\gamma)$	Potential energy	Collective potential energy.
$\hat{H}_{\text{coll}}$	Collective Hamiltonian	Total collective Hamiltonian.
$\langle IMK\|$	Bra in lab frame	Left eigenstate in the laboratory frame.
$\|IMK\rangle$	Ket in lab frame	Right eigenstate in the laboratory frame.
$\Psi_{\alpha IM}(\beta,\gamma,\Omega)$	Combined wave function	Total wave function depending on β, γ and Euler angles Ω.
Ω	Euler angles	Set of Euler angles: (α, β, γ).
$D^I_{MK}(\Omega)$	Wigner D-function	Wigner D-function for rotation.
$d^I_{MK}(\beta)$	Wigner small-d function	Wigner small-d function (depends on β).
$\Phi_{\alpha IK}(\beta,\gamma)$	Vibrational wave function	Vibrational part in the intrinsic frame.
$E_{\alpha I}$	Energy eigenvalue	Collective energy eigenvalue.
$F_L^J(q)$	Form factor	Electromagnetic form factor of multipolarity L.
q	Momentum transfer	Magnitude of momentum transfer.
Z	Proton number	Atomic number (number of protons).
J_i, J_f	Initial and final multipolarities	Multipolarities of the initial and final states.
T^J_λ	Multipole operator	Spherical tensor operator of rank λ.
$OBDM^{J_i,J_f}_{ab}(\lambda,\mu_i\|\tau_\alpha,b)$	One-body density matrix	Transition one-body density matrix element.
a, b	Single-particle states	Indices of single-particle states.
μ_i	Isospin projection	$+1/2$ (proton) or $-1/2$ (neutron).

3. Result and Discussion

The NushellX@MSU code was used to perform these calculations. The (HO) functions are Waves Functions for a single particle. the Bohr-Mottelson (BO) model was used. For the 5/2 transition, the magnetic shape factors were calculated for the ^{19}O isotope. Possible su3sd in the sd shell.

Magnetic form factors of the ^{19}O nucleus isotope were calculated. The possibility (su3sd) in the Sd shell for the 5/2 transition. Figure1 shows the magnetic form factors M1, M3, and M5 A function of motion transport for the 5/2 state for the ^{19}O nucleus. The red curve shows the magnetic shape factor M1. The maximum values of the scattered electron scattering for the magnetic shape factor M1 are close to of motion transport values q = 0.3 f m^{-1}, 1.6 fm^{-1}, and 2.8 f m^{-1}, the minimum values of the scattering are at q = 1 fm^{-1} and 2.4 fm^{-1}. The blue curve shows the magnetic form factor M3, the maximum scattering values of scattered electrons for magnetic shape factor M3 are close to the impetus transport amounts. q = 0.9 f m^{-1}, 2.3 fm^{-1}. The minimum scattering value is at q = 1.5 fm^{-1}, 3.4 fm^{-1}. The green curve shows the magnetic shape factor M5, the maximum scattering values of scattered electrons for magnetic shape factor M5 are close to of motion transport values. q = 1.8 fm^{-1}. The minimum scattering value is q=3.4 fm^{-1}. The black curve shows the sum of magnetic form factors M1, M3, M5. The dominant component is M1. The dominance of the M1 contribution indicates that the magnetic dipole transition is the principal mechanism governing the electron scattering process in this nucleus. The relatively small contributions of M3 and M5 suggest weaker higher-order magnetic multiple excitations[21]. The decrease of the form factor at larger momentum transfer reflects the finite spatial distribution of nuclear magnetization.

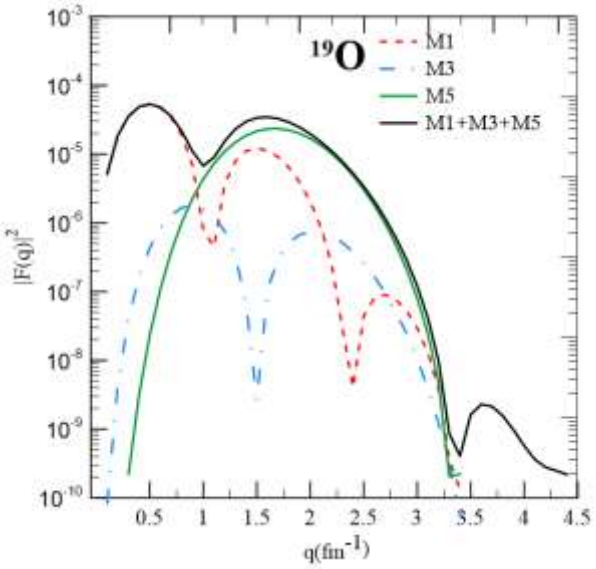


Figure 1. Magnetic form factors of an isotope ^{19}O using the Bohr-Mottelson (BM) model with the potential Skyrme-type Hamiltonian (skx) to the 5/2 state.

The magnetic form factors for the ^{17}O isotope were calculated. The possibility of su3sd in the sd shell for the 5/2 transition. Figure2 shows the magnetic form factors M1, M3 and M5 of motion transport for the 5/2 state for the ^{17}O nuclei. The red curve shows the magnetic shape factor M1. The maximum values of scattered electron scattering for the magnetic form factor M1 are close to the values of the momentum transport q = 0.6 f m^{-1}, 1.7 fm^{-1}, and 3.1 fm^{-1}, the minimum values of scattering are at q = 1.3 fm^{-1} and 2.4 fm^{-1}, 2.1, fm^{-1}. The black curve shows the magnetic shape factor M3, the maximum values of scattered electron scattering for the magnetic form factor M3 are close to the amounts of the impetus transport. q = 1.3 fm^{-1} and 2.8 fm^{-1}. The minimum value of scattering is at q = 2.3 fm^{-1}, 4.4 fm^{-1}. The green curve shows the magnetic form factor M5, the maximum values of scattered electron scattering for the magnetic shape factor M5 are close to the values of the momentum transport. q = 2 fm^{-1}. The minimum value of scattering is q=4.4 fm^{-1}. The blue curve represents the sum of the magnetic shape factors M1, M3, and M5. The dominant component is M1. The agreement between theoretical and experimental results confirms the suitability of the Bohr–Mottelson collective model and the adopted shell-model configuration for describing the magnetic structure of the ^{17}O nucleus. The M1 component remains dominant throughout most of the momentum-transfer region.

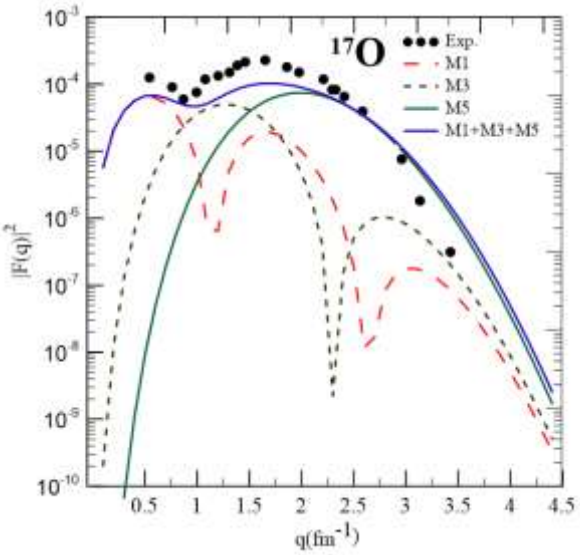


Figure 2. Magnetic form factors of an isotope ^{17}O using the Bohr-Mottelson (BM) model with Harmonic oscillator (HO) potential to the 5/2 state. Experimental results are taken from Ref [21-24].

Figure 3. shows the distribution of the magnetic form function of the ^{25}Al nucleus in terms of the transport vector q, which represents the amount of momentum transferred in the reaction. The red line shows the sum of the values of M1, M3 and M5. At low values of q (less than 1 fm^{-1}), the contribution of M1 is relatively large. At moderate values of q (about 1.5 fm^{-1}), the contribution of M3 and M5 is clearly visible. At higher values of q (greater than 2.5 fm^{-1}), the values decrease, indicating the disappearance of the magnetic effect of the nucleus in this transmitted momentum range. The noticeable contribution of M3 and M5 at intermediate momentum transfer indicates the participation of higher-order magnetic excitations. However, the M1 component remains the largest contribution to the total magnetic form factor.

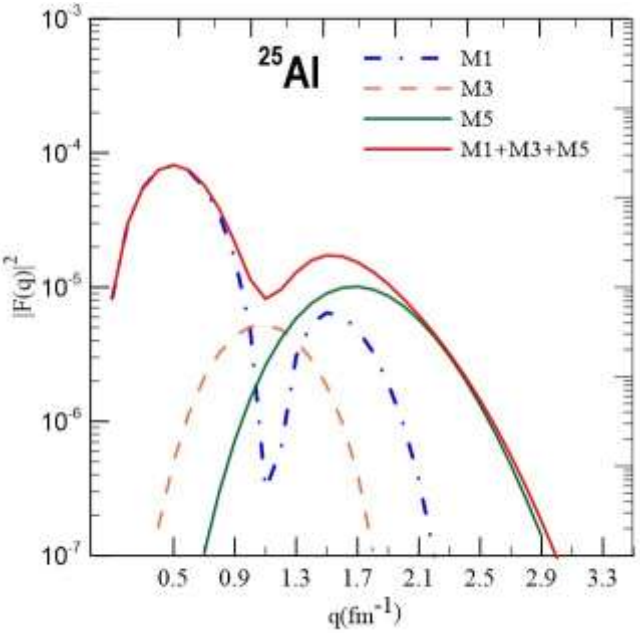


Figure 3. Magnetic form factors of an isotope ^{25}Al using the Bohr-Mottelson (BM) model with Harmonic oscillator (HO) potential to the 5/2 state.

4. Conclusion

The magnetic electron scattering form factors of the ^{17}O, ^{19}O, and ^{25}Al nuclei were calculated using the Bohr–Mottelson collective model within the SDPF shell-model space. The contributions of the M1, M3, and M5 magnetic multiples were investigated for the selected transitions. The results showed that the M1 component is the dominant contribution to the total magnetic form factor in all studied nuclei, while the M3 and M5 components provide smaller but non-negligible contributions at intermediate momentum transfer values. A satisfactory agreement between the calculated and experimental data was obtained for the ^{17}O nucleus, demonstrating the reliability of the adopted model. The present calculations provide useful information about the magnetic structure and collective behavior of sd-shell nuclei and confirm the applicability of the Bohr–Mottelson model in describing electron scattering observe.

References

1. R. Naik, "Studying fusion reactions for effect of P (CN) on heavy nucleus formation and for nuclear structure effects." Oregon State University, 2007.
2. K. Matsuyanagi, M. Matsuo, T. Nakatsukasa, K. Yoshida, N. Hinohara, and K. Sato, "Microscopic derivation of the Bohr-Mottelson collective Hamiltonian and its application to quadrupole shape dynamics," Phys Scr, vol. 91, no. 6, pp. 1–62, 2016, doi: 10.1088/0031-8949/91/6/063014.
3. R. Roy and B. P. Nigam. "Nuclear Physics Theory and Experiment", John and Sons, New York (1967).
4. B. A. Brown, R. Radhi, and B. H. Wildenthal, “Electric quadrupole and hexadecupole nuclear excitations from the perspectives of electron scattering and modern shell-model theory,” Phys Rep, vol. 101, no. 5, pp. 313–358, 1983.
5. H. Sagawa and B. A. Brown, "E2 core polarization for sd-shell single-particle states calculated with a skyrme-type interaction," Nucl Phys A, vol. 430, no. 1, pp. 84–98, 1984.

6. H. Uberall, "Electron Scattering from Complex Nuclei " Academic Press, (2012).
7. K. S. Jassim and H. A. Kassim, "Core Polarization Effects of some odd sd-shell nuclei using M3Y effective nucleon-nucleon interaction," Romanian Journal of Physics, vol. 58, no. 3–4, pp. 319–329, 2013.
8. Jassim, K.S., Faris, A.I., Nuclear structure of ^{60}Ni nucleus using shell model calculations, Journal of Computational and Theoretical Nanoscience, 14(5), 2336–2340,2017.
9. M. L. Adnan and K. S. Jassim, "The Bohr-Mottelson model was used to calculate the longitudinal form factor of ^{31}P, ^{27}Al, and ^{23}Na nuclei," in AIP Conference Proceedings, 2023. doi: 10.1063/5.0161520
10. Mosel, U., and Gallmeister, K. (2024). Lepton-induced reactions on nuclei in a wide kinematical regime. Physical Review D, 109(3), 033008.
11. Franco-Munoz, T., González-Jiménez, R., and Udías, J. M. (2025). Effects of two-body currents in the one-particle one-hole electromagnetic responses within a relativistic model. Journal of Physics G: Nuclear and Particle Physics, 52(2), 025103.B. A. Brown, "Lecture notes in nuclear structure physics," National Super Conducting Cyclotron Laboratory, 2005.
12. Rahaman, U. (2026). Shape transitions and ground-state properties of tungsten isotopes in covariant density functional theory: U Rahaman. Indian Journal of Physics, 1-14.
13. B. A. Brown, "Lecture notes in nuclear structure physics," National Super Conducting Cyclotron Laboratory, 2005.
14. K. S. Krane and D. Halliday," Introductory nuclear physics". Wiley New York, 1988.
15. A. Hasan and D. Hamed, "Journal of Kufa-Physics," Vol. 5, No.2, 2013.
16. A. N. Bohr and B. R. Mottelson, "Nuclear Structure (in 2 volumes)." World Scientific Publishing Company, 1998.
17. A. Bohr and B. R. Mottelson, "Nuclear deformations." WA Benjamin, 1975.
18. B. Mottelson, "Nobel Prize lecture," Rev. Mod. Phys, vol. 48, p. 375, 1976.
19. de Forest Jr, T., and Walecka, J. D. (1966)." Electron scattering and nuclear structure". Advances in Physics, 15(57), 1-109.
20. K, Kumar, and Baranger, M. (1967). "Complete numerical solution of Bohr's collective Hamiltonian". Nuclear Physics A, 92(3), 608-652.
21. T. W. Donnelly and J. D. Walecka, "Elastic magnetic electron scattering and nuclear moments," Nucl Phys A, vol. 201, no. 1, pp. 81–106, 1973.
22. P. J. B. and P. W. M. Glaudemans, "Shell-model applications in nuclear spectroscopy." North-Holland Pub. Co., 1977.
23. T. W. Donnelly, and I. Sick, (1984). "Elastic magnetic electron scattering from nuclei." Reviews of modern physics, 56(3), 461.
24. M. V. Hynes, H. Miska, , Norum, B., Bertozzi, W., Kowalski, S., Rad, F. N., ... and Berman, B. L. (1979). “Electron Scattering from the Ground-State Magnetization Distribution of O17.” Physical Review Letters, 42(22), 1444.